



Thermodynamic, transport and mechanical properties of amorphous metallic alloys: Relation to the glass transition

Livio Battezzati

Dipartimento di Chimica IFM e Centro di Eccellenza NIS, Università di Torino, Via P. Giuria 7, 10125 Torino, Italy

ARTICLE INFO

Article history:

Received 4 July 2008

Accepted 7 October 2009

Available online 6 November 2009

Keywords:

Metallic glasses

Amorphous materials

Thermodynamic properties

Mechanical properties

ABSTRACT

Properties related to the glass transition of metallic melts are reviewed both on empirical ground and using the statistics of local minima in the potential energy landscape of the material. For metallic alloys some correlations have been disputed (e.g., the one between the Kauzmann and VFT temperatures). In the first part of this report these issues are considered and the possible reasons for either good or poor correlation are outlined.

Then the relationship of the glass transition to mechanical properties (e.g., strength, moduli) is described with special attention to the failure mechanism of amorphous alloys via shear band propagation. The relationships are discussed for glass-forming alloys in comparison also with properties of other families of glass-formers.

© 2009 Elsevier B.V. All rights reserved.

1. Introduction

The glass transition is the key phenomenon determining properties for glassy materials. It is usually described in terms of transport (e.g., viscosity) and/or thermodynamic quantities (e.g., heat capacity in the undercooling regime, excess enthalpy and entropy) [1]. Glass forming liquids can be classified according to their strength or, alternatively, fragility. The fragility is expressed by parameters related to the rate with which some liquid properties change on cooling. In an Arrhenius plot the viscosity of a strong liquid increases almost linearly with decreasing temperature, contrary to the viscosity of a fragile liquid which is low at high temperature and increases fast when approaching the glass transition [2]. In terms of the potential energy landscape (PEL) model, different activation barriers must be overcome for accessing the various inherent structures of the liquid. These differ in number and correspond to energy minima of different depth whose sampling depend on temperature [3]. A manifestation of this is that the extensive thermodynamic quantities change on undercooling. Further indication of the sampling of various landscape configurations is that fragile liquids loose entropy faster than strong ones when approaching the glass transition [4].

It is well established that mechanical properties of metallic glasses correlate with the glass transition temperature, T_g [5,6]. There have been also attempts of correlating the fragility of melts with elastic properties of the corresponding glass, namely the Poisson ratio, although they did not provide a stringent test of the

relationship [7]. The link with the glass transition is, however, well evidenced by considering the energetics of shear bands. Their propagation has been discussed having in mind a mechanism of mechanical failure starting with a shear offset event causing a local temperature rise above T_g , the maturation of the shear band to end up in a final crack [8]. This is reviewed here for metallic glasses in comparison also with properties of other families of glass-formers.

2. Viscosity and fragility

The glass transition is conventionally defined as the temperature at which the melt viscosity, η , reaches the value of 10^{12} Pa s. For glass-formers it displays non-linear dependence on inverse temperature and is most often described by the VFT equation [1,2]:

$$\eta = A \exp \left[\frac{B}{(T - T_0)} \right] \quad (1)$$

where A and B are constants and T_0 is the temperature where the viscosity should diverge in case the melt could be cooled below T_g . The fragility parameter m is defined as

$$m = \left[\frac{d(\log \eta)}{d(T_g/T)} \right]_{T=T_g} \quad (2)$$

and the slope of an Arrhenius plot of Eq. (1) at T_g gives

$$m = \frac{BT_g}{2.3(T_g - T_0)^2} \quad (3)$$

Observing that the viscosity of glass-formers can span about 17 orders of magnitude from the above melting point ($\log \eta = -5$) to

E-mail address: livio.battezzati@unito.it.

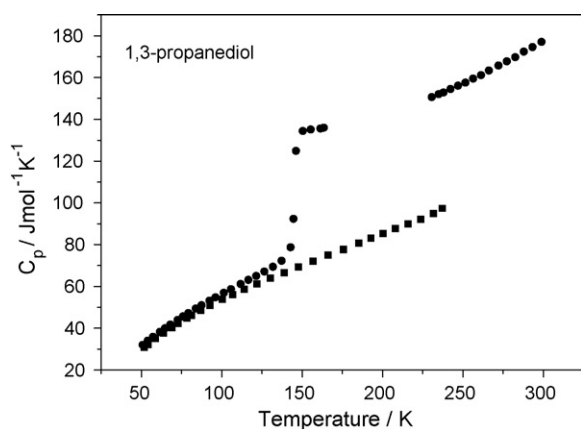


Fig. 1. The specific heat of 1,3-propanediol as a function of temperature. Squares: crystal phase and circles: glass and liquid phases. Data from Ref. [10].

the glass transition ($\log \eta = 12$), Angell and Martinez [9] have introduced a kinetic fragility index defined as

$$F_{\text{kin},1/2} = \frac{2T_g}{T_{1/2}} - 1 \quad (4)$$

where $T_{1/2}$ is the temperature at which $\log \eta$ is half way the above range ($\log \eta = 3.5$). As expected the $F_{\text{kin},1/2}$ parameter scales with the m index for metallic and other glass-formers of low/intermediate strength. For very strong melts $T_{1/2}$ can hardly be reached and the fragility parameter is then used as $F_{\text{kin},3/4}$ with $T_{3/4}$ as the relevant temperature.

3. Thermodynamics and fragility

Thermodynamic analyses of glass-formers in the undercooling regime show high values of the excess specific heat of the liquid with respect to the crystal, $\Delta C_p = C_{p,l} - C_{p,x}$ until the T_g is reached. Examples are reported in Figs. 1 and 2, respectively for an organic substance, 1,3-propanediol [10], and a metallic alloy, $\text{Pd}_{77.5}\text{Cu}_6\text{Si}_{16.5}$ [11]. The jump in specific heat at T_g for the glass and T_m for the crystal is well apparent. The specific heat of the crystalline phases has an increasing monotonic trend, the specific heat of the glass is close to that of the crystal until the glass transition is reached and the undercooled liquid is accessed. The specific heat just above T_g can be fitted with a single function with that

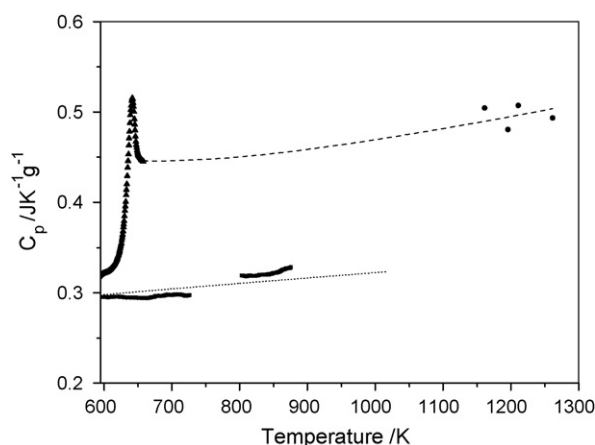


Fig. 2. The specific heat of $\text{Pd}_{77.5}\text{Cu}_6\text{Si}_{16.5}$ as a function of temperature. Squares: crystal phase, triangles: glass, and circles: liquid. The lines are fit to liquid data (dashed), weighed average of specific heat of components (dashed). Data from Ref. [11].

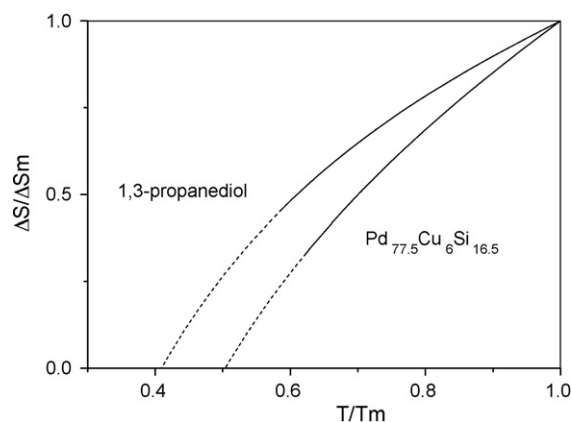


Fig. 3. The reduced entropy difference between undercooled liquid and crystal phases as a function of reduced temperature for 1,3-propanediol and $\text{Pd}_{77.5}\text{Cu}_6\text{Si}_{16.5}$. The dashed line is the extrapolation of experimental data to $\Delta S = 0$.

of the liquid at high temperature. Knowing the specific heat of all phases, extensive thermodynamic functions can be determined as a function of temperature. Fig. 3 shows the entropy difference between liquid and crystal, ΔS , for the two cases. The loss of liquid entropy with respect to that of the crystal is slightly higher for the metallic alloy. The temperature range accessible to measurements terminates at T_g . Extrapolating the data to $\Delta S = 0$ the Kauzmann temperature is identified where the two phases would have the same entropy, i.e., a hypothetical state for the liquid. For the plot in Fig. 2 the crystal as reference state is used. In order to express better the melt fragility in thermodynamic terms, the rate of entropy loss as a function of temperature has been plotted as $\Delta S_g / \Delta S$ versus T_g / T where ΔS_g is the excess entropy at T_g (Fig. 4). Such plot is comparable with that of viscosity referred to Section 1 above, therefore, a fragility parameter, $F_{\text{td},1/2}$ analogous to the $F_{\text{kin},1/2}$ defined with Eq. (4), has been introduced [9]. The two parameters correlate rather strictly for various glass-formers [9] whereas for metallic alloys the correlation cannot be proven with certainty because of the paucity of data available and their experimental scatter [1]. As an example, the m parameter determined from viscosity and relaxation kinetic measurements for propanediols [12] and $\text{Pd}_{77.5}\text{Cu}_6\text{Si}_{16.5}$ [11] are of the order of 52 and 58–65, respectively. The $F_{\text{td},3/4}$ parameters are 0.64 and 0.84, respectively, much more different than the m s.

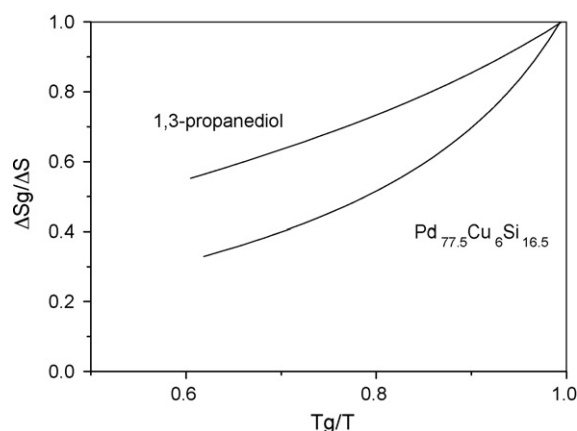


Fig. 4. The Angell's thermodynamic fragility plot of $\Delta S_g / \Delta S$ versus T_g / T for 1,3-propanediol and $\text{Pd}_{77.5}\text{Cu}_6\text{Si}_{16.5}$. The lower slope at T_g indicate stronger behaviour of 1,3-propanediol.

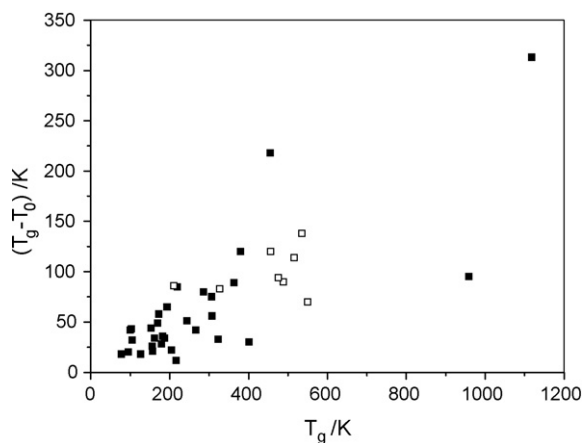


Fig. 5. The $(T_g - T_0)$ difference versus T_g for various glass-formers. Full symbols: inorganic and organic glasses, data from Ref. [12]. Open symbols: metallic glasses, data from Ref. [1].

4. Relationship between parameters

Considering the empirical relationships among the fragility parameters m , $F_{i,1/2}$ and $F_{i,1/2}$ for various types of glasses the existence of a correlation between kinetic and thermodynamic fragility can be surmised as stated in the Adam–Gibbs entropy model of viscosity [1–3]. This has the direct consequence of relating the T_0 and T_K temperatures. This is checked in the following with respect to T_g since it is expected the fragility of melts is directly related to the difference between T_g and T_0 (or possibly T_K). Due to the temperature dependence of viscosity, the difference $(T_g - T_0)$ must be substantial in strong melts and, in the limit of an Arrhenian behaviour, T_0 is nil. On the other hand, such difference must reduce in relative terms in more fragile melts. Fig. 5 shows $(T_g - T_0)$ versus T_g for various glass-formers with evidence for the metallic ones. For a given T_g , the span of $(T_g - T_0)$ is actually relevant reflecting the difference in fragility of melts. Considering now T_K , it is reported versus T_0 in Fig. 6 for the organic and inorganic glass-formers listed in [12] and for metallic glasses. In general, the two temperatures appear strictly correlated for substances as diverse as light organic molecules (low temperature range) and silicates (high temperature range). The larger deviation from the equality of the two temperatures is found for metallic glasses where T_0 appears frequently lower than T_K . Whether this is a sign of different behaviour with respect to other glass-formers, or an effect of scatter of data, remains to be estab-

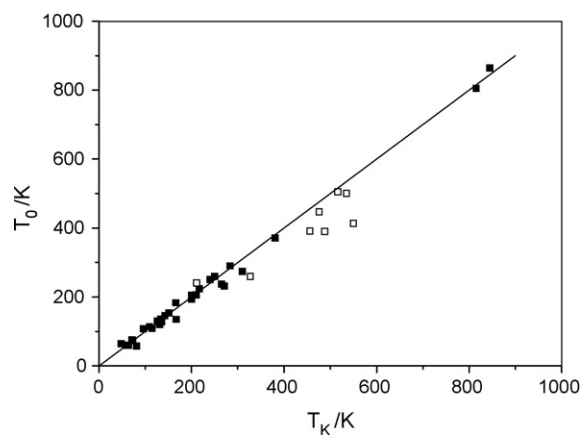


Fig. 6. Plot of T_0 versus T_K . The line is drawn according to $T_0 = T_K$. Full symbols: inorganic and organic glasses, data from Ref. [12]. Open symbols: metallic glasses, data from Ref. [1].

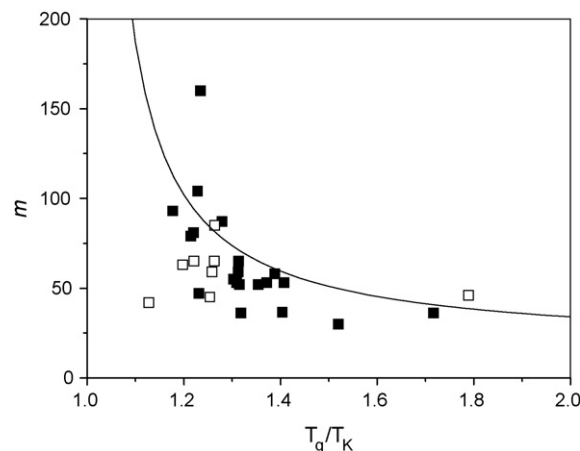


Fig. 7. The fragility index m for metallic (open symbols [1]) and non-metallic (full symbols [4]) as a function of the ratio T_g/T_K . Line computed using Eq. (5).

lished. Apart from the unavoidable difficulty both in measurements of viscosity and specific heat, it is noted here that the reference state for T_K is the corresponding crystal which is clearly defined for molecular substances and for some silicates, but in almost all cases does not exist as such for metallic alloys for which the equilibrium constitution is a mixture of phases. This is an inherent problem in obtaining a comparable T_K for metallic alloys.

A different view has recently been put forward with specific reference to metallic glasses, in addition to other substances, for which it has been suggested on the basis of a model expressing changes in bond ordering in the liquid, that the ratio T_0/T_K is not constant and equal to 1, but scales with the m parameter [13].

The PEL model provides further insight into this issue. The number of local minima which can be accessed by melt configurations and their energy distribution, determines the configurational entropy of the liquid. The energy distribution of minima can be expressed by means of various functions (for a summary, see Ref. [3]). Considering that the configurational specific heat of the liquid, which is usually approximated by the difference between liquid and crystal phases, ΔC_p , has often a hyperbolic dependence on temperature, the hyperbolic distribution of energies only will be used here from which a simple expression for the fragility index, m , is arrived at [3]

$$m = 17 \frac{T_g}{T_g - T_K} \quad (5)$$

A plot of m versus T_g/T_K is shown in Fig. 7 for inorganic, organic and metallic glasses, providing further confirmation that metallic glasses conform to the general trend of glass-formers and that they rank among fragile-intermediate melts. The use of another energy distribution, i.e., gaussian, gives similar trend so that the present experimental data do not allow to discriminate between models [3,14].

5. Glass transition and mechanical properties

The correlation of mechanical properties of metallic glasses with the glass transition temperature in first instance reflects the dependence of mechanical properties on cohesive energy and hence melting point of the solid. In fact, T_g occurs for different glasses at a fraction of the melting point comprised approximately between 1/2 and 2/3. It has been noted that part of the scatter in the plots of moduli and strength versus T_g can actually be related to the varied proportionality between T_g and T_m [15].

Here we compare further (Figs. 8 and 9, respectively) the Young's modulus, E , and the hardness, H_v , of practically all known metal-

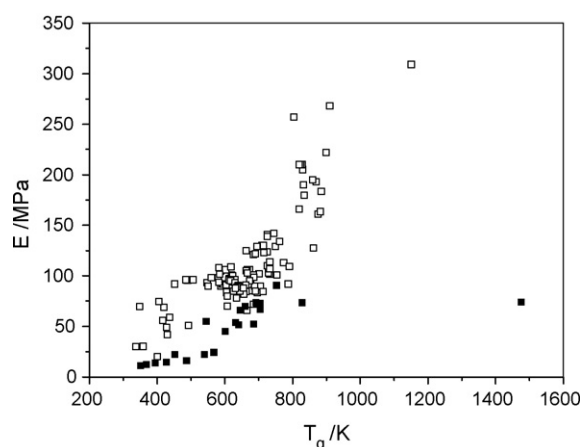


Fig. 8. The plot of Young's modulus versus T_g for metallic glasses (open symbols [15]) and inorganic glasses (full symbols [16]).

lic glasses obtained both in ribbon and bulk form with those of selected inorganic glass-formers (selenides, borates, silicates, phosphates). The data have been collected from various sources [4,15,16]. The hardness is taken here as a measure of the strength of the glasses. The well established relationship between hardness and yield stress has been discussed for metallic glasses with indentation models and yield criteria [17]. Again, the broad correlation between E , H_v and T_g is confirmed but it is observed that the correlation is better defined within each family of materials.

Glasses, including metallic, do not strain harden, unlike crystalline metals, but at temperatures far enough from T_g , fail at high stresses. For metallic glasses the theoretical limit is approached. The failure is due to inhomogeneous flow due to strain localization in thin shear bands [5]. The correlation of strength parameters, with the glass transition temperature shows that there a link can be established between thermal and mechanical properties of glasses, specifically those leading to fracture. This has been sought for metallic glasses by considering the volumetric energy content of the material at yielding (and most often at fracture) as expressed by its resilience, $R = \sigma_y^2/2E$, with σ_y the yield strength. The observation of fracture surfaces evidences vein and river patterns [5,6], filaments and drops [18]. This shows that zones of the glassy material reach the liquid state and, consequently, temperatures in excess of T_g . The amount of alloy involved in such heating has been estimated by computing the thermal energy needed to reach T_g from the temperature at which the mechanical test is performed, usually

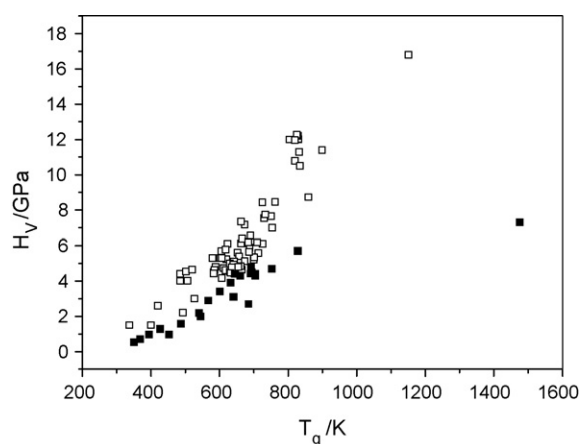


Fig. 9. The plot of hardness versus T_g for metallic glasses (open symbols [15]) and inorganic glasses (full symbols [16]).

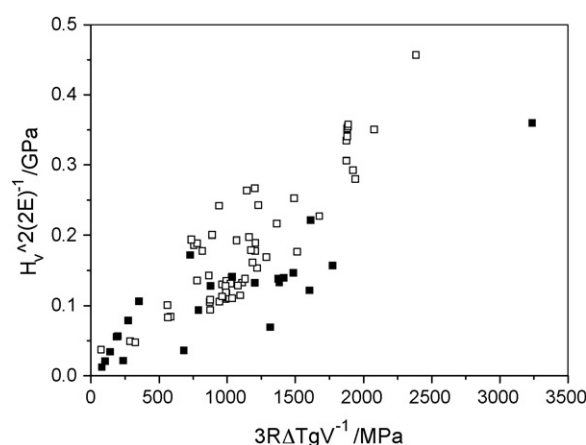


Fig. 10. The square of the hardness divided by the elastic modulus versus the volumetric amount of heat needed to bring the material from room to the glass transition temperature. Metallic glasses (open symbols [15]) and inorganic glasses (full symbols [16]). Among the latter the points for selenides are aligned at the left of the plot.

ambient temperature T_a , $E_t \approx \int_{T_a}^{T_g} \frac{C_p}{V} dT$ with V the molar volume and C_p the molar specific heat, and comparing it with the amount of energy released elastically. To overcome the lack of experimental data, both ρ and C_p were taken as constants as in a previous analysis [19], and C_p taken as $3R$, R being the gas constant, with the justification that this underestimates the actual values of only about 10%. Then, the thermal energy becomes $E_t \approx 3R\Delta T_g/V$. The resilience of metallic glasses versus the thermal energy showed a clear correlation implying that shear band propagation is related to the glass transition in that local temperature rise occurs after a shear offset event and the shear band becomes operative, behaves like a crack releasing elastic energy. The microstructural length scale where these events occur were shown to be compatible with the size of the molten zone in fusible coating experiments [20] and of veins and other features on the fracture surfaces of metallic glasses. To complete the comparison with other glasses, a plot of the quantity $H_v^2/2E$ is reported versus E_t in Fig. 10 of course noting that the values in the ordinate do not bear a meaning in terms of energy beyond the relationship between hardness and yield stress. The overall correlation is much less than for metallic glasses alone. However, it clearly exists for the family of selenide glasses indicating a common mechanism for failure again related to the glass transition. Points for other glasses (e.g., borates and phosphates) do not have a similar correlation and a different mechanism of failure can be suggested.

6. Conclusions

This contribution has reviewed the fragility parameters of both kinetic and thermodynamic origin for glasses of various types and discussed the extent of their correlation as well as possible causes of discrepancies.

The hyperbolic distribution of energies in a potential energy landscape of the liquid provides a simple mean of expressing the m parameter versus T_g/T_K showing that metallic glasses conform to the general trend of glass-formers and that they rank among fragile-intermediate melts.

The relationship between the Young's modulus and hardness and T_g has been discussed observing that the correlation can be defined with some confidence within each type of glassy materials.

Issues related to the temperature rise during shear band propagation in metallic glasses have finally been reviewed underlining the general correlation between the resilience (elastic energy

stored at fracture) and the amount of thermal energy released. This relationship appear to apply to some families of glasses whereas other types apparently fracture with a different mechanism.

Acknowledgments

Work performed for “Progetto D23, Bando Regionale Ricerca Scientifica Applicata 2004.” Thermophysical properties of melts are studied within the Thermolab Project of ESA.

References

- [1] L. Battezzati, A. Castellero, P. Rizzi, J. Non-Cryst. Sol. 353 (2007) 3318.
- [2] C.A. Angell, Science 267 (1995) 1924–1935.
- [3] G. Ruocco, F. Sciortino, F. Zamponi, C. De Michele, T. Scopigno, J. Chem. Phys. 120 (2004) 10666.
- [4] L. Battezzati, G.M.M. Mortarino, J. Alloys Compd 483 (2009) 222–226.
- [5] C.A. Schuh, T.C. Hufnagel, U. Ramamurty, Acta Mater. 55 (2007) 4067.
- [6] A.R. Yavari, J.J. Lewandowski, J. Eckert, MRS Bull. 32 (2007) 635.
- [7] L. Battezzati, Mater. Trans. 46 (2005) 2915.
- [8] L. Battezzati, D. Baldissin, Scripta Mater. 59 (2008) 223–226.
- [9] L.-M. Martinez, C.A. Angell, Nature 410 (2001) 663.
- [10] K. Takeda, O. Yamamuro, I. Tsukushi, T. Matsuo, H. Suga, J. Mol. Struct. 479 (1999) 227–235.
- [11] G.L. Fiore, L. Battezzati, Rev. Adv. Mater. Sci 18 (2) (2008) 190–192.
- [12] C.A. Angell, J. Res. Natl. Inst. Stand. Technol. 102 (1997) 171–185.
- [13] H. Tanaka, J. Non-Cryst. Sol. 351 (2005) 678–690.
- [14] L. Battezzati, Rev. Adv. Mater. Sci 18 (2) (2008) 184–189.
- [15] L. Battezzati, D. Baldissin, M. Baricco, T. Aycan Baser, D. Firrao, P. Matteis, G.M.M. Mortarino, Mater. Res. Soc. Symp. Proc. 1048 (2008), 1048-Z02-08.
- [16] L. Battezzati, D. Baldissin, A. Habib, P. Rizzi, J. Phys. Conf. Ser. 144 (2009) 012088.
- [17] V. Keryvin, Acta Mater. 55 (2007) 2565–2578.
- [18] P. Rizzi, L. Battezzati, J. Non-Cryst. Sol. 344 (2004) 94.
- [19] B. Yang, C.T. Liu, T.G. Nieh, Appl. Phys. Lett. 88 (2006) 221911.
- [20] Y. Zhang, N.A. Stelmashenko, Z.H. Barber, W.H. Wang, J.J. Lewandowski, A.L. Greer, J. Mater. Res. 22 (2007) 419–427.